Available online at www.sciencedirect.com

Journal of the European Ceramic Society 24 (2004) 1603–1606

www.elsevier.com/locate/jeurceramsoc

Influence of cation substitution on the phase formation kinetics of $Sr_{0.7}Bi_{2.3}Ta_2O_9$ thin films

Woo-Chul Kwak, Yun-Mo Sung*

Functional Nanostructured Materials Laboratory (FNML), Department of Materials Science and Engineering, Daejin University, Pochun-koon, Kyunggi-do 487-711, South Korea

Abstract

The Ta^{5+} ions in sol-gel derived $Sr_{0.7}Bi_{23}Ta_2O_9$(SBT) thin films were partially substituted by Zr^{4+} to form $Sr_{0.7}Bi_{2.3}Ta_{1.7}Zr_{0.3}0_9$ (SBTZ) thin films and Aurivillius phase formation characteristics were compared for each thin film. X-ray diffraction (XRD) analyses were performed on the thin films heated in the range of 730–760 °C at 10 °C intervals and it was found that phase formation and crystal growth were greatly affected by the film composition and crystallization temperature. Johnson–Mehl–Avrami (JMA) isothermal kinetic analyses were performed on the XRD results and activation energy and Avrami exponent values were determined for the fluorite-to-Aurivillus phase transformation. A reduction of ~82 kJ/mol in activation energy was observed for the SBTZ thin films, which revealing the key reason of enhanced kinetics in SBTZ. XRD and scanning electron microscopy (SEM) showed the remaining of fluorite phase in SBT and the formation of a secondary phase in SBTZ.

Keywords: Films; Kinetics; Perovskite; Sol-gel process; X-ray methods

1. Introduction

$SrBi_2Ta_2O_9$ (SBT) is one of the most promising materials for non-volatile ferroelectric random-access memory (NvFeRAM) applications because of its excellent fatigue resistance up to $\sim 10^{-12}$ switching cycles, low coercive field performance and low leakage current densities on Pt electrodes.[1,2] However, the application of SBT thin films has been limited due to the low remanent polarization (P_r) and high processing temperature (~800 °C). Recently, Cao et al.[3–5] reported improved ferroelectric properties of cation-doped (La^{3+}, Ca^{2+} for Sr^{2+} and V^{5+} and Nb5+ for Ta^{5+}) SBT thin films. Also, Desu et al.[6,7] have investigated the solid solution of $0.7SrBi_{2.3}Ta_2O_9$–$0.3Bi_3TaTiO_9$ (SBT-BTT), which is equivalent to $Sr_{0.7}Bi_{2.3}Ta_{1.7}Ti_{0.3}O_9$ and reported increased P_r and decreased crystallization temperature. However, the basic reason for the reduction in the processing temperature by cation doping or solid solution formation was not investigated in detail.

In this study, an attempt has been made to reveal the origin of lowered crystallization temperature in cation-doped SBT ferroelectric thin films compared to SBT. In detail, the influence of partial substitution of Ta^{5+} sites by Zr^{4+} ions on the crystallization characteristics of $Sr_{0.7}Bi_{2.3}Ta_2O_9$ has been analyzed using isothermal kinetic analyses.

2. Experimental procedure

In the preparation of SBTZ sol, Zr-isopropoxide was dissolved in Ta-methoxyethoxide by refluxing at 130 °C and the solution was distilled. And then, this Ta–Zr methoxyethoxide was added to the Sr–Bi methoxyethoxide solution and the final Sr–Bi–Ta–Zr methoxyethoxide solution was prepared. The SBT and SBTZ thin films were prepared on a $Pt/Ti/SiO_2/Si$ wafer using spin coating at a spin speed of 3000 rpm for 30 s. The film was dried in air for 1 mm followed by heat-treating at 150 °C for 5 mm and pyrolysis at 450 °C for 10 min order to remove the organics. The coating process was repeated several times in order to achieve the desired thickness of ~400 nm. The SBT and SBTZ thin films prepared were further heat treated at 600 °C for 1 h to complete the fluorite formation. To investigate the fluorite-to-Aurivillius phase transformation characteristics

---

* Corresponding author. Fax: +82-31-539-1980.
E-mail address: ymsung@road.daejin.ac.kr (Y.-M. Sung).

0955-2219/03/$ - see front matter
doi:10.1016/S0955-2219(03)00396-0

for the above films, the films were further annealed in the temperature range of 730–760 °C at 10 °C intervals by giving soaking time as 4–80 min. The X-ray diffraction (XRD: Rigaku-Ultima 2000, Tokyo, Japan) was performed using a precision thin film attachment. XRD patterns of these films were recorded and the volume fraction values (x_A) of fluorite-to-Aurivillius phase transformation were obtained. To obtain respective integrated intensity, a multi-peak separation program (MDI Jade 5.0, Materials Data, Inc., Livermore, CA, USA) was used. An isothermal kinetic study has been carried out using these volume fraction values. Scanning electron microscopy (SEM: Philips XL-30 E-SEM, Eindhoven, The Netherlands) was used to examine the crystal morphology of thin films.

3. Results

Fig. 1 shows the X-ray diffraction patterns of the SBT and SBTZ thin films heated at 740 °C for different time intervals. As the soaking time increases, the gradual conversion of fluorite-to-Aurivillius phase transformation takes place in both the cases. However, the conversion rate in the SBTZ thin films was much higher than that in the SBT thin films. Even after heated for 80 min at 740 °C SBT films still show a remaining fluorite phase. On the other hand SBTZ films show the formation of a small amount of secondary phase and its relative intensity seems to increase with temperature as shown in Fig. 1. The XRD integrated intensity of the secondary phase peak was deleted from that of the Aurivillius (105) peak for the following volume fraction calculation. The volume fraction of phase transformation (x_A) from fluorite to Aurivillius was determined using a conventional XRD quantitative analysis method.[8–10] The volume fraction values were applied to the isothermal Johnson–Mehl–Avrami (JMA) kinetic equation.[11]

$$x_A = 1 - \exp(-kt)^n \tag{1}$$

$$\ln[-\ln(1 - x_A)]_T = n \ln k + n \ln t \tag{2}$$

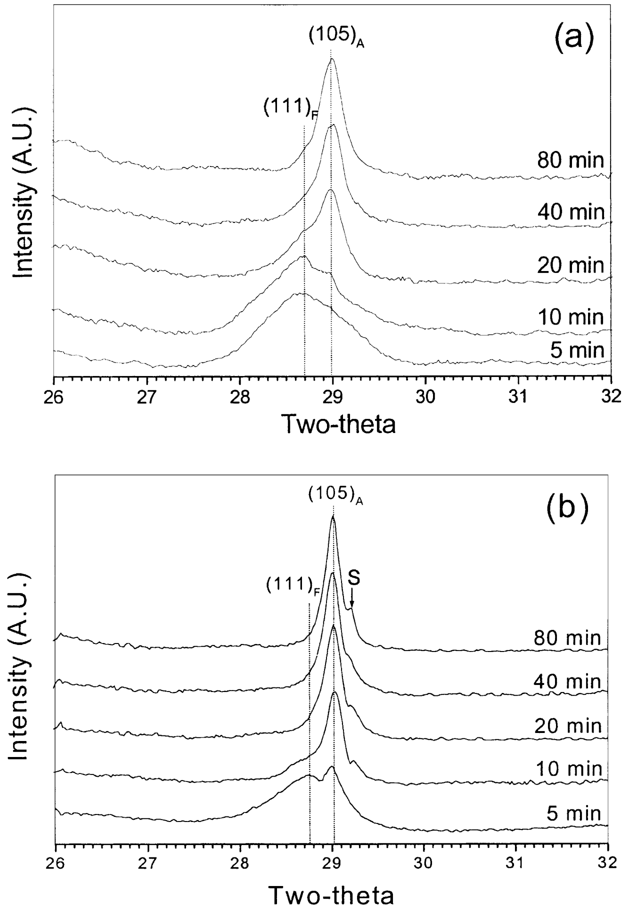

Fig. 1. X-ray diffraction (XRD) patterns of (a) SBT and (b) SBTZ thin films on Pt/Ti/SiO_2/Si substrates heated at 740 °C. Here, $(105)_A$,$(111)_F$ and S denote the reflections from Aurivillius (105), fluorite (111) and a secondary phase, respectively.

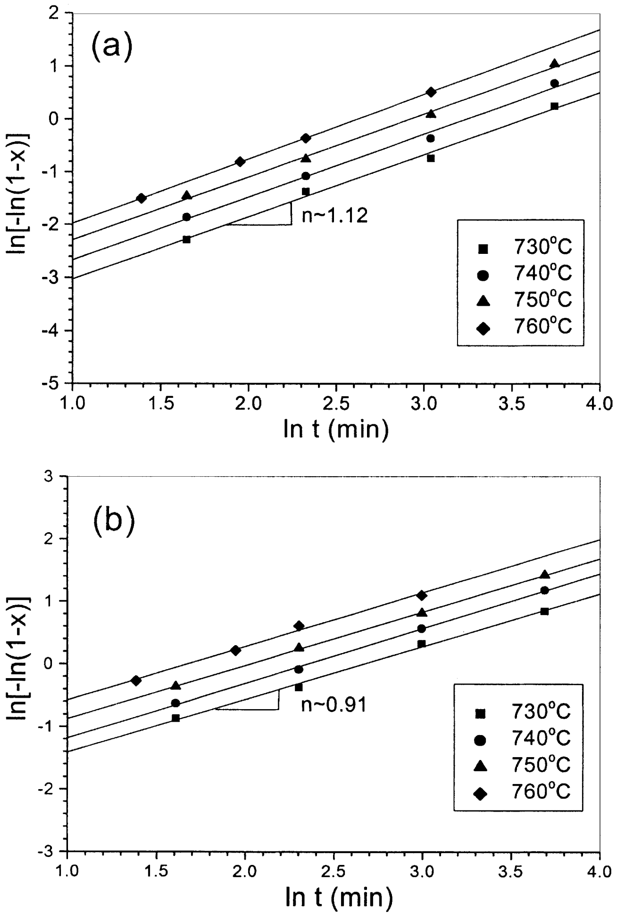

Fig. 2. JMA plots for the Aurivillius phase formation of (a) SBT and (b) SBTZ thin films.

where, x_A is the volume fraction transformed at a particular temperature, T is the temperature, t is the time, k is the reaction rate constant and n is the Avrami exponent. The Avrami exponent, n, can be calculated from the slopes of the curves in $\ln[-\ln(1-x)]$ vs. $\ln t$ plot. The temperatures used in the present study were 730, 740, 750 and 760 °C, and as shown in Fig. 2, the Avrami exponent values were determined as ~1.12 and ~0.91 for the fluorite-to-Aurivillius phase transformation in SBT and SBTZ, respectively.

The activation energies of SBT and SBTZ thin films were also determined using the γ-intercept values of $n \ln k$ and following Arrhenius equation was applied.

$$\ln k = \ln k_o - \frac{Q}{RT} \qquad (3)$$

Here, k_o is the pre-exponential constant, R is the gas constant, and Q is the activation energy. As shown in Fig. 3, from the slopes of the curves, the activation energy values for the SBT and SBTZ thin films for the Aurivillius phase formation were found to be ~264 and ~182 kJ/mol, respectively.

In Fig. 4 SEM images of both the SBT and SBTZ thin films heat treated at 760 °C for 40 min reveal formation of worm-like crystals on the Pt substrates. Also, SBT films show locally inhomogeneous microstructure and SBTZ show clusters of very fine crystals between elongated Aunvillius crystals.

4. Discussion

The higher peak intensity and smaller full width at half maximum (FWHM) in XRD patterns indicate a better crystallinity and well-developed surface microstructure for the SBTZ thin films, compared to its counterpart. Aurivillius phase is formed through an intermediate phase known as fluorite and the phase transformation from fluorite to Aurivillius includes a certain amount of cations dissociated with oxygen ions. Ionic bond strength of Sr–O is ~134 kJ/mol[12] and those of Bi–O and Ta–O were approximated to ~190 and ~365 kJ/mol, respectively using the linear relationship between the ionic field strength and the bond strength.[12] According to our recent study on SBT and SBTZ powders the activation energy associated with the formation of the Aurivillius phase was determined as ~375 and ~281 kJ/mol, respectively. Since the activation energy value of SBT is comparable to the energy value associated with the dissociation of Ta–O bonds (~365 kJ/mol), it can be stated that intensive dissociation of Ta–O bonds must be the controlling mechanism for the phase transformation. Similarly, it can be stated that in the SBTZ system, the activation energy (~281 kJ/mol) involved for the transformation is associated with the dissociation of Zr–O bonds (~256 kJ/mol). In the SBTZ system, the Ta^{5+} sites are partially occupied by Zr^{4+} ions. Subsequently during the heat treatment, the breaking of Zr–O ions takes place at a lower temperature. Therefore, the rearrangement and phase transformation to the final phase take place, resulting in a low

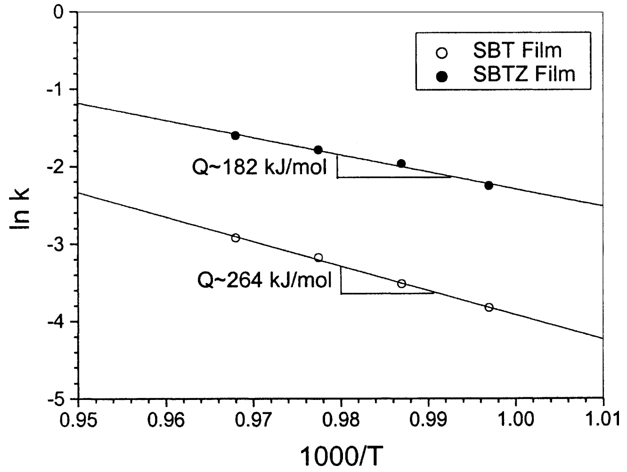

Fig. 3. Arrhenius plots of Aurivillius phase formation in SBT and SBTZ thin films.

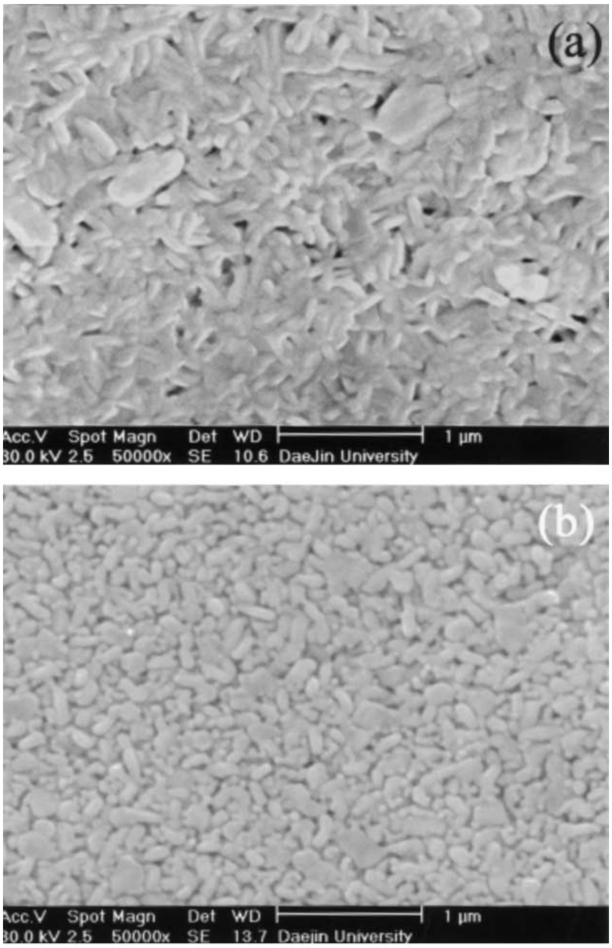

Fig. 4. SEM secondary electron images of (a) SBT and (b) SBTZ thin films heated at 760 °C for 40 min.

temperature phase formation in the SBTZ. In the present study, the activation energy values, associated with the formation of Aurivillius phase from thin films of SBT and SBTZ system, are calculated to be ~264 and ~182 kJ/mol respectively. In this case, also it can be seen that the activation energy is much less for the SBTZ system, suggesting the same mechanism for the films as well. The low activation energy values associated with films in comparison to powder seem to be related with the internal energy accumulated in the film during drying and annealing.

The Avrami exponents, indicating the nucleation and crystal growth modes, were determined as ~1.12 and ~0.91 for the fluorite-to-Aurivillius phase transformation in the SBT and SBTZ. These Avrami exponent values can be analyzed by following relationship:[12]

$$n = a + mb \tag{4}$$

where a refers to the nucleation rate during crystal growth with the value of 1 for a constant nucleation rate, 0 for a zero nucleation rate, $a > 1$ for an increasing nucleation rate and $a < 1$ for a decreasing nucleation rate; m corresponds to the dimensionality of crystal growth; and b relates to the mechanism of crystal growth with the value of 1.0 for an interface-controlled process and 0.5 for a diffusion-controlled process. The fluorite-to-Aurivillius phase transformation involves intensive dissociation of ionic bonds and diffusion of the cations and thus $b = 0.5$. Then, there are two possibilities; one is $a = 0.5$ and $m = 1$ and the other is a = 0 and $m = 2$.

The morphological features of the SBT film annealed at 760 °C for 40 min show a locally inhomogeneous microstructure, possibly with fluorite-type crystals. Therefore, an annealing time of 40 min would not be sufficient to completely transform the SBT film into the Aurivillius phase. In contrast, the surface morphology of the SBTZ films at the same annealing temperature and time shows a well developed dense grain structure with an average grain size of ~300 mm. However, in the case of SBTZ the formation of very fine secondary phase was found. The Aurivillius grains show worm-like morphology in both the films indicating almost one-dimensional crystal growth, which implies that the decreased nucleation rate with diffusion-controlled crystal growth is the crystal growth mechanism during the fluorite-to-Aurivillius phase formation.

5. Conclusions

The crystallization kinetics of sol-gel derived SBT and SBTZ thin films were studied. From the X-ray diffraction results, the activation energy for Aurivillius formation in SBT and SBTZ thin films were determined as ~264 and ~182 kJ/mol, respectively. The reduced activation energy in SBTZ thin films is associated with the low dissociation energy of the Zr–O bonds, which replace the Ta–O bonds. Thus, it can be concluded that the lowered crystallization temperature in SBTZ thin films is originated from the reduced activation energy for the fluorite-to-Aurivillius phase transformation. The Avrami exponent values were determined as approximately 1.0 for both SBT and SBTZ thin films, indicating one-dimensional crystal growth with a diffusion-controlled mechanism at a decreasing nucleation rate. The remaining fluorite phase was found in SBT films and the formation of small amount of secondary phase was identified in SBTZ.

Acknowledgements

This work was supported by grant No. (R05-2001-000-00810-0) from the Basic Research Program of the Korea Science & Engineering Foundation (KOSEF).

References

1. Araujo, C. A., Cuchiaro, J. D., McMillan, L. D., Scott, M. C. and Scott, J. F., Fatigue-free ferroelectric capacitors with platinum electrodes. *Nature*, 1995, **374**, 627–629.
2. Zhu, Y., Desu, S. B., Li, T., Ramanathan, S. and Nagata, M., $SrBi_2Ta_2O_9$ thin films made by liquid source metal-organic chemical vapor deposition. *J. Mater. Res.*, 1997, **17**, 783–792.
3. Wu, Y. and Cao, G. Z., Enhanced ferroelectric properties and lowered processing temperatures of strontium bismuth niobates with vanadium doping. *Appl. Phys. Lett.*, 1999, **75**, 2650–2652.
4. Forbess, M. J., Seraji, S., Wu, Y., Nguyen, C. P. and Cao, G. Z., Dielectric properties of layered perovskite $Sr_{1-x}A_xBi_2Nb_2O_9$ ferroelectrics (A = La, Ca and x = O, 0.1). *Appl. Phys. Lett.*, 2000, **76**, 2934–2936.
5. Wu, Y., Forbess, M. J., Seraji, S., Limmer, S. J., Chou, T. P. and Cao, G. Z., Oxygen-vacancy-related dielectric relaxation in $SrBi_2Ta_{1.8}V_{0.2}O_9$ ferroelectrics. *J. Appl. Phys.*, 2001, **89**, 5647–5652.
6. Zhu, J., Zhang, X., Zhu, Y. and Desu, S. B., Size effects of $0.8SrBi_2Ta_2O_9$–$0.2Bi_3TiNbO_9$ thin films. *J. Appl. Phys.*, 1998, **83**, 1610–1612.
7. Ryu, S. U., Tirumala, S., Joshi, P. C. and Desu, S. B., Fabrication and characterization of $(1-x)SrBi_2Ta_2U_9$–xBi_3TaTiO_9 layered structure solid solution thin films for ferroelectnc random access memory (FRAM) applications. *Thin Solid Films*, 1999, **340**, 53–61.
8. Toraya, H., Yoshimura, M. and Somiya, S., Calibration curve for quantitative analysis of the monoclinic-tetragonal ZrO_2 system by x-ray diffraction. *J. Am. Ceram. Soc.*, 1984, **67**, C–l19-C-121.
9. Schmid, H. K., Quantitative analysis of polymorphic mixes of zirconia by X-ray diffraction. *J. Am. Ceram. Soc.*, 1987, **70**, 367–376.
10. Sung, Y.-M., Nonisothermal phase formation kinetics in sol-gel-derived strontium bismuth tantalite. *J. Mater. Res.*, 2001, **16**, 2039–2044.
11. Avrami, M., Kinetics of phase change I: general theory. *J. Chem. Phys.*, 1939, **7**, 1103–1112.
12. Kingery, W. D., Bowen, H. K. and Uhlman, D. R., *Introduction to Ceramics,* 2nd edn. John Wiley and Sons, New York, 1976.